

Characterizing Vacuum Facility Backpressure Effects on the Performance of a Hall Thruster^{*†}

Richard R. Hofer
richard@hofer.com

Peter Y. Peterson
pypeters@engin.umich.edu

Alec D. Gallimore
alec.gallimore@umich.edu

Plasmadynamics and Electric Propulsion Laboratory
Department of Aerospace Engineering
University of Michigan
College of Engineering
Ann Arbor, MI 48109 USA

IEPC-01-045

Vacuum facility backpressure is known to affect the performance of Hall thrusters through ingestion of background gases by the thruster. Ingested gases may be ionized and subsequently accelerated, artificially increasing the measured thrust. This study seeks to characterize how backpressure affects performance by changing the pumping speed of the facility, not by the commonly used technique of bleeding additional propellant in to the vacuum chamber. Performance is measured at xenon pumping speeds of 140,000 and 240,000 l/s, on a nominally 5 kW Hall thruster at voltages and flow rates of 300-600 V and 5-15 mg/s. At the highest pumping speed, performance data are collected while matching the discharge current observed at the lower pumping speed. Thrust, specific impulse, and efficiency are presented at both pumping rates. The anode mass flow at zero backpressure is calculated by extrapolation from the observed change in flow rate with pressure. On average, the correction is 4% of the anode flow rate at the maximum pumping speed, which is comparable to the uncertainty in the flow controllers.

Introduction

Because of their combination of high specific impulse (I_{sp}), efficiency, and thrust density, the Hall effect thruster (HET) can significantly enhance a variety of space missions by increasing mission life or payload mass for a given amount of propellant, or by reducing initial spacecraft mass when ΔV or payload requirements are fixed. These features either enable space missions to occur by providing sufficient performance that is otherwise unattainable, or enhance space missions by reducing trip time and/or launch costs through decreased spacecraft mass.

The HET is a coaxial device in which a magnetic field that is produced by an electromagnet is channeled between an inner ferromagnetic core (pole piece) and outer ferromagnetic ring (Figure 1). This configuration results in an *essentially* radial magnetic field with a peak strength of a few hundred Gauss.

This field strength is such that only the electrons are magnetized. In addition, an axial electric field is provided by applying a voltage between the anode and the downstream cathode. As electrons migrate upstream from the cathode to the anode, the $\mathbf{E} \times \mathbf{B}$ action on the electrons causes them to drift in the azimuthal direction, forming a Hall current. Through collisions, these electrons ionize propellant molecules, which are injected through the anode. The ionized propellant molecules are accelerated by the axial electric field to provide thrust. The mixture of electrons and ions in the acceleration zone means that the plasma is electrically neutral, and as such, is not space-charge limited in ion current (thrust) density. Since the magnetic field suppresses the axial mobility of the electrons while exerting essentially no effect directly on the ion motion, the plasma can support an axial electric field with a potential difference close to the applied voltage between the electrodes. Thus, the bulk of the ions are accelerated to kinetic energies to

^{*} Presented as Paper IEPC-01-045 at the 27th International Electric Propulsion Conference, Pasadena, CA, 15-19 October 2001.

[†] Copyright © 2001 by the Electric Rocket Propulsion Society. All rights reserved.

within 85% of the applied discharge voltage.^{1,2} This combination of processes accounts for the HETs high thrust efficiency.

HETs come primarily in two variants: the stationary plasma thruster (SPT) (also known as the magnet layer thruster) and the anode layer thruster (TAL). The main difference between these two devices is that the SPT uses a dielectric coating that usually contains boron nitride to electrically insulate its acceleration channel while the TAL uses channels made from metal. Performance characteristics of both engines are virtually identical. Although they vary in size and input power, HETs that are currently being considered for station-keeping typically operate at discharge voltages of 300 to 350 V, and thruster currents between 4.5 and 15 A, with xenon mass flow rates of 5 to 15 mg/s. Recent interest in multi-mode operation for orbit-raising and station-keeping is driving the performance requirements of next-generation HETs.³ However, the thruster power level (and therefore the current and mass flow rates) that will be needed in the future for both commercial and government space missions will be considerably higher.

Space missions that will require significantly higher HET power levels include many of those being considered in NASA's Human Exploration and Development of Space (HEDS) program. For example, NASA has embarked on a program under the auspices of HEDS to develop high-power HETs for a variety of missions including a piloted expedition to Mars within the next few decades.⁴ One scenario for a piloted mission to Mars uses a Solar Electric Propulsion (SEP) stage to raise a chemically-powered Mars Transfer (MT) stage to a highly elliptical orbit around the Earth. Once the MT stage is in the proper orbit, the crew uses a small, chemically-propelled vehicle to rendezvous with it. When the crew is in place and the MT stage has been certified, it separates from the SEP stage and ignites its engines for the trip to Mars.⁵ This scenario reduces both trip time (for the crew) and initial spacecraft mass by utilizing a high-performance SEP stage for much of the ΔV . Moreover, since the SEP stage operates in proximity to the Earth, nuclear power is not needed for this mission.

The key to developing the SEP stage is the utilization of powerful engines that possess high exhaust velocity, high thrust efficiency, and a wide range of exhaust

velocities (*i.e.*, capable of multi-mode operation). To this end, the NASA Glenn Research Center initiated a program to design a 50-kW-class HET, the NASA 457M, by the end of calendar year 2001 and to test this engine next year.⁶ While NASA's eventual goal in terms of power for an individual thruster that would be used in a cluster to propel the Mars SEP stage has yet to be identified, given the fact that the propulsion system for this stage must process hundreds of kilowatts to several megawatts of power, power levels in excess of 100 kW are not unreasonable.

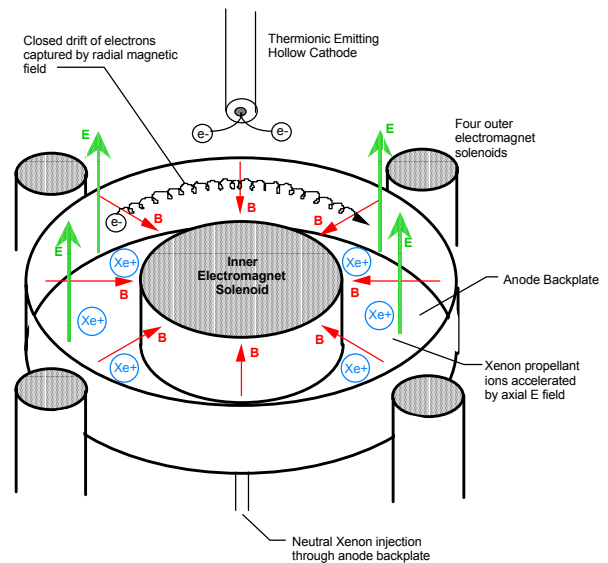


Figure 1 – Schematic of a HET.

Although HETs have performance characteristics that make them attractive for a variety of missions, the complex nature of their operation is a source of concern from a spacecraft integration point-of-view. HETs experience discharge chamber wall erosion due to sputtering from energetic ions near the exit of the discharge chamber.⁷ Deposition of eroded thruster material on sensitive spacecraft surfaces (*e.g.*, solar arrays and optics) may pose a threat to spacecraft health. While numerous studies have taken place to characterize the above processes on the ground,^{8,9,10,11} what complicates these endeavors is the fact that facility effects have been shown to have a profound impact on these investigations. Improper matching of engine test goals with a facility can render a series of experiments meaningless. For example, if the chamber is too small, its boundaries (walls) can affect measurements by altering the flowfield or by introducing contaminants due to tank wall erosion.

Material sputtered from tank walls can interfere with measurements that use witness plates, collimated samples, and QCMs to predict thruster and spacecraft material erosion. The electrical conductivity of tank walls in proximity to the engine (*i.e.*, within 1 m) has been shown to influence the electric field in the plume and the plume flow field.¹²

If the tank pressure is too high, HET operation may be influenced by ingestion of the background chamber molecules. This effect artificially increases the propellant mass flow rate of the engine, resulting in performance and operation changes consistent with the increased number of propellant particles. Furthermore, plume diagnostic experiments can be affected. A large partial pressure of background gas molecules can affect ion current density and energy distribution measurements by artificially increasing the local charge density through charge exchange collisions.

While there are no universally-accepted guidelines on facility pressure for HET testing, Randolph, *et al.*¹³ suggest that in order to characterize a HET in terms of performance, electromagnetic interference (EMI), far-field (≤ 1.2 m) plume properties, and life, the vacuum chamber pressure should be no more than 5×10^{-5} , 5×10^{-5} , 1×10^{-5} , and 5×10^{-6} Torr, respectively. Since the pressures at low Earth orbit and at geosynchronous orbit are approximately 5×10^{-6} and 5×10^{-10} Torr, respectively, a perfect simulation of pressure is not necessary. Randolph based his analysis on free-molecular flow, arguing that below a certain chamber pressure, thruster operating characteristics are not affected by the random flux of vacuum chamber particles. Conversely, if a thruster is tested above the specified pressure, the influence of background gas being ingested into the engine through free-molecular flow must be taken into account when analyzing test data. However, since Randolph based his pressure estimates on 1-kW-class thrusters where the internal pressure is expected to be approximately 5×10^{-4} Torr,¹⁴ it stands to reason that still lower pressures would be needed for high-power thrusters where internal pressures are lower according to HET scaling laws.¹⁵ If we conserve the ratio of thruster discharge chamber pressure, as determined by HET scaling laws, and tank pressure, we find that Randolph's estimates may be a factor of five too high for 50 kW engines. Thus, there is a need to understand how facility effects

(*e.g.*, chamber pressure) influence the operation of HETs over a wide range of thruster power levels.

The University of Michigan's Plasmadynamics and Electric Propulsion Laboratory (PEPL) has embarked on such a program. Our goal is to investigate the role of facility effects on HET performance, plume parameters, life, and spacecraft contamination. This paper will concentrate on analyzing performance data collected on a 5-kW-class HET at two facility pumping speeds. Future investigations will extend the analysis to higher power thrusters. The results will be presented after the thruster and experimental facilities are described. Another paper given in these proceedings describes experiments conducted at PEPL that characterized the ion current density profile of a HET with nude and collimated Faraday probes.¹⁶

Experimental Apparatus

All experiments were conducted on the 5-kW-class laboratory model P5 Hall thruster. The P5 was developed by PEPL and the Air Force Research Laboratory to serve as a test-bed for new diagnostics and for investigating Hall thruster processes. Depicted in Figure 2, the P5 has an outer diameter of 173 mm, a channel width of 25 mm, and a channel depth of 38 mm. While the nominal operating power level of the P5 is 5 kW, the engine is capable of sustained operation above 9 kW. A more detailed description of the P5 can be found in Ref. 17.

All experiments were made in PEPL's Large Vacuum Test Facility (LVTF). The LVTF is 9 meters long by 6 meters in diameter and is pumped by up to seven LN₂-cooled CVI TM1200 reentrant (nude) cryopumps. The seven nude cryopumps, which are equivalent to fourteen large (1.2-m-diameter) cryotubs in terms of pumping speed, give the LVTF an overall pumping speed of 500,000 l/s on nitrogen and over 240,000 l/s on xenon. The base pressure of the LVTF is less than 2×10^{-7} Torr. One of the benefits of using a large vacuum facility with a modular pumping system is the ability to vary background chamber pressure by altering pumping speed. Figure 3 shows tank pressure versus thruster power (at 300 V) as a function of how many LVTF nude cryopumps are in operation. The use of varying chamber pumping speed to study tank pressure effects is superior to elevating chamber

pressure by auxiliary gas injection from a standpoint of cost (if xenon is used as the auxiliary gas), and by avoiding issues associated as to where in the facility the auxiliary gas is introduced and what influence non-xenon auxiliary gas (to reduce cost) has on HET operation.

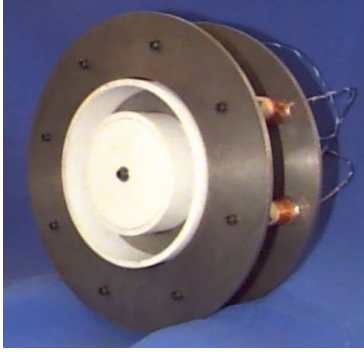


Figure 2 – Photograph of the P5 HET.

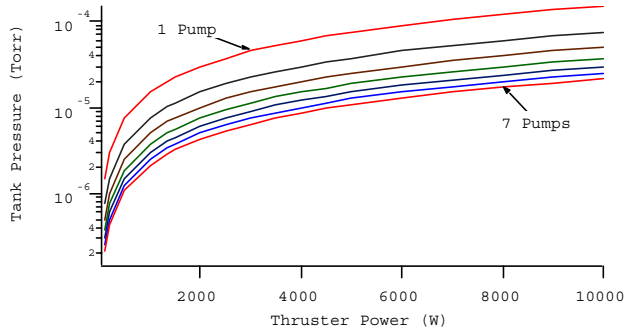


Figure 3 – LVTF pressure vs. thruster power (@ 300 V) with 1 - 7 pumps operating.

Chamber pressure was monitored using two hot-cathode ionization gauges as indicated in Figure 4. The first gauge was a Varian model 571 gauge with a HPS model 919 Hot Cathode Controller. The second is a Varian model UHV-24 nude gauge with a Varian UHV senTorr Vacuum Gauge Controller. Pressure measurements from both gauges were corrected for xenon using the known base pressure on air and a correction factor of 2.87 for xenon according to the following equation,¹⁸

$$P_c = \frac{P_i - P_b}{2.87} + P_b \quad (1)$$

Where P_c is the corrected pressure on xenon, P_b is the base pressure, and P_i is the indicated pressure when xenon is flowing into the vacuum chamber.

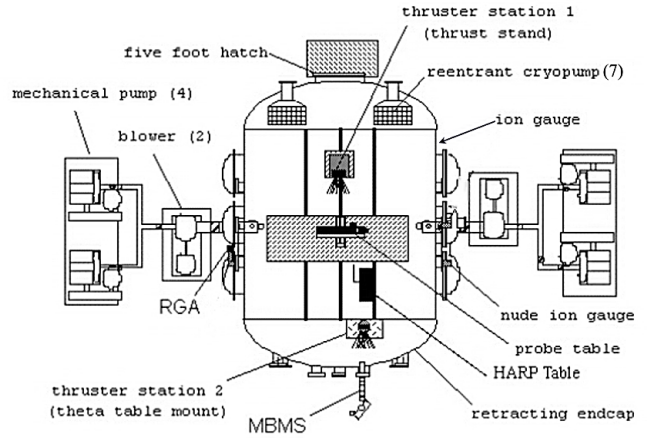


Figure 4 – Schematic of the LVTF.

High-purity (99.999% pure) xenon propellant was supplied to the P5 through stainless-steel feed lines with 20 and 200 sccm MKS Model 1100 Mass Flow Controllers calibrated for xenon. The controllers were calibrated using the ideal gas law, the time rate of change of the pressure and temperature in a known volume, and the compressibility of xenon. The system is accurate to within 1-2% of the indicated value on the anode flow controller and 3-4% on the cathode flow controller.

Performance measurements were made with an inverted pendulum type thrust stand, based on the GRC design. A Lucas Schaevitz model 100-HR Linear Variable Differential Transformer (LVDT), which has a resolution of 2.5×10^{-3} mm, is used to measure deflection of the pendulum. Output from the LVDT is read by a Lucas Schaevitz DTR-451 Digital Transducer Readout that in turn outputs a voltage to a strip chart recorder. The thrust stand inclination is monitored by a Spectron Systems Technology MUPI-2 inclinometer. A stepper motor is used to level the stand *in situ*. Another motor is employed to turn a pulley system that deploys weights to provide *in situ* calibrations. During testing, a calibration is typically preformed prior and after thrust measurements to minimize the error that could occur due to thermal drift of the thrust stand. To reduce the influence of thermal drift, a water-cooled shroud encompasses the components of the thrust stand. The overall error observed during the experiments was ± 1 mN.

Results and Discussion

To quantify how the backpressure affects the performance of a HET in the LVTF, the facility was operated at two different pumping speeds. Specifically, either four or seven cryopumps were operated, corresponding to pumping speeds of approximately 140,000 l/s (on xenon) and 240,000 l/s. Figure 5 plots the pressure in the facility versus the total xenon mass flow into the chamber. The percentage pressure drop is also shown, indicating that switching from four to seven cryopumps results in a 41% drop in pressure on average over the flow rates of interest.

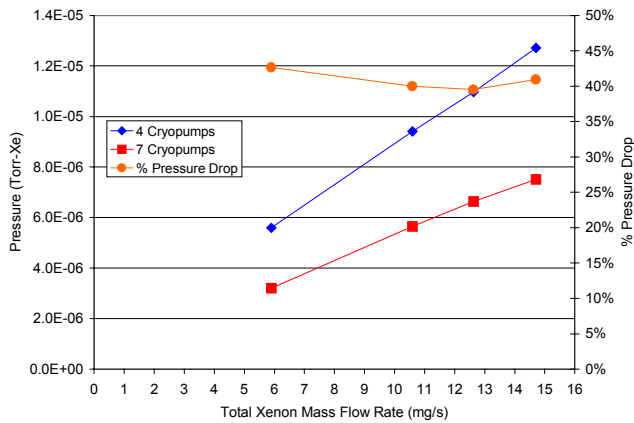


Figure 5 – LVTF pressure as a function of the total xenon mass flow rate into the chamber. The percentage pressure drop is also shown versus flow rate.

Performance of the thruster was first evaluated with 4 pumps operating. The remaining pumps were then turned on and the experiments were repeated. When operating the thruster with 7 pumps, the anode mass flow rate was increased so that the discharge current matched what was observed with 4 pumps. During 7 pump operation, the currents to the inner and outer magnets were set to the values used with 4 pumps operating. Keeping the magnets constant is done because the discharge current in a HET can be extremely sensitive to the coil currents depending on operating point. For example, it is always possible to increase the discharge current by changing the magnets off their optimum values. So when the pressure is lowered, the discharge current of the high pressure condition can be matched without changing

the anode mass flow rate. The electron current and ion current are changing under these conditions, not the amount of neutral ingestion.

What influence keeping the magnetic field constant with a changing backpressure has on thruster operation is not well understood. For example, it is not known how this affects the ionization and acceleration processes and near-field plume structure. This could be vitally important for thrusters with ionization and acceleration occurring downstream of the exit plane. Unfortunately, there does not seem to be any obvious way to change both the flow rate and the magnetic field without the resulting measurement being arbitrary.

Tables A-1 and A-2 in the appendix show the performance of the P5 when 4 or 7 cryopumps are operating in the LVTF, respectively. Figures 6-8 plot thrust, anode I_{sp} , and anode efficiency versus discharge voltage at constant current and 4 or 7 cryopumps operating. The figures span 300-600 V in 100 V steps and discharge currents of 5, 10, 12.5, and 15.1 A. Figures 9-11 plot the thrust, anode I_{sp} , and anode efficiency versus the discharge current at constant voltage and 4 or 7 cryopumps.

Matching the discharge current at different pumping speeds is expected to also match the measured thrust. This is not the case in the figures, where it is shown that for all but the 15.1 A conditions that the thrust is actually higher when all 7 cryopumps are operating. On average, the thrust is 4-5 mN higher for the 5, 10, and 12.5 A conditions. These differences are greater than the resolution of the thrust stand, which was ± 1 mN in these experiments. The magnetic field configuration, interaction of the plume with the background gases, or unknown systematic error in the experiment are possible causes for the observed trends in the thrust. Further investigations of these trends are planned.

I_{sp} and efficiency also exhibit similar trends as the thrust, but because the mass flow rate was always increased at the high pumping speed, the differences are not as large. For the 5 A cases, the differences are about 50 s and 3% higher at the high pumping speed for the I_{sp} and efficiency, respectively. At 10 and 12.5 A, I_{sp} and efficiency are approximately the same. The expected trend, lower I_{sp} and efficiency at the high

pumping speed, is only consistently so at 15.1 A. The observed differences are within the uncertainty of I_{sp} and efficiency (4-5%). This suggests that performance measurements in the LVTF are an accurate depiction of on-orbit performance at either of the pumping speeds for mass flow rates up to 15 mg/s. Future investigations are planned to characterize the facility at flow rates above 15 mg/s.

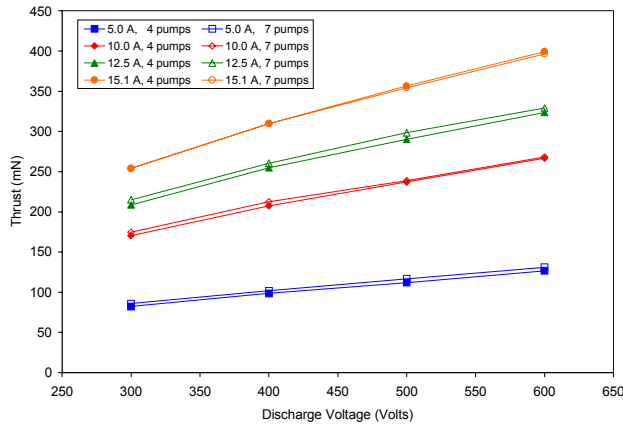


Figure 6 – Thrust versus discharge voltage for 4 or 7 cryopump operation at constant discharge current.

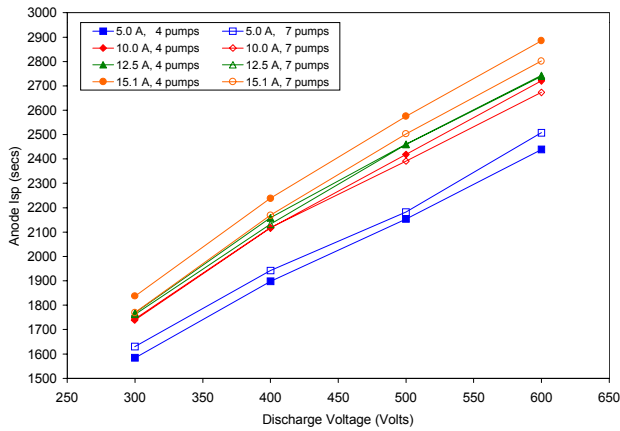


Figure 7 – Anode specific impulse versus discharge voltage for 4 or 7 cryopump operation at constant discharge current.

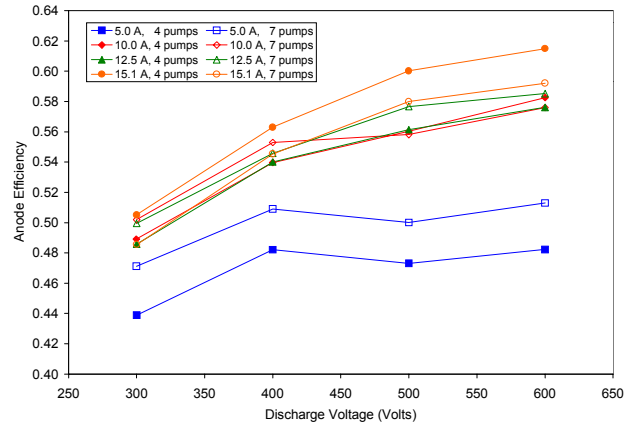


Figure 8 – Anode efficiency versus discharge voltage for 4 or 7 cryopump operation at constant discharge current.

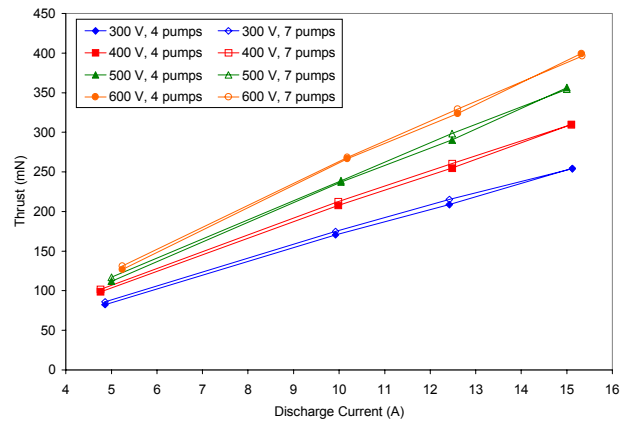


Figure 9 – Thrust versus discharge current for 4 or 7 cryopump operation at constant discharge voltage.

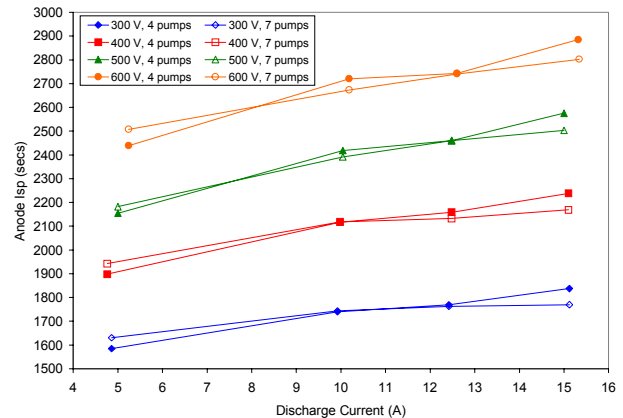


Figure 10 – Anode specific impulse versus discharge current for 4 or 7 cryopump operation at constant discharge voltage.

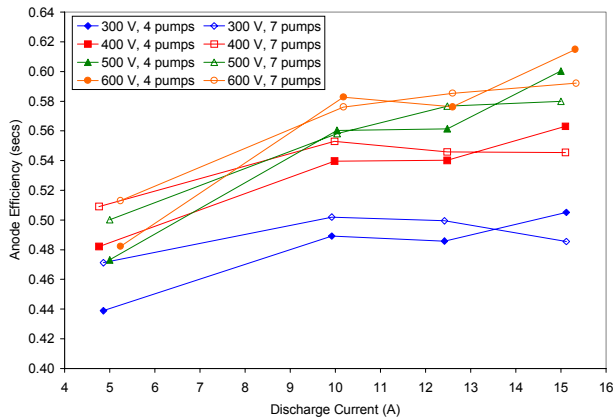


Figure 11 – Anode efficiency versus discharge current for 4 or 7 cryopump operation at constant discharge voltage.

Figures 12-15 plot the anode mass flow versus the chamber pressure for each of the discharge currents that were investigated. Linear curve fits are used to extrapolate the data to zero background pressure so that an estimation of the vacuum anode mass flow rate can be made. Table 1 presents the results of these extrapolations for each discharge current that was investigated. The vacuum anode flow rates are shown to increase with decreasing pressure, as expected. For a given discharge current, the dependence on the discharge voltage appears to be random and is used to estimate the error. An average error in determining the correction is estimated as 30%. The corrections are on average 4% of the anode flow rate when 7 cryopumps were operating, which is on the order of the uncertainty in the flow controllers. With 4 cryopumps running, the corrections are on average 6% of the anode flow rate. Randolph's criteria for performance was based off a comparison between the percentage uncertainty in the mass flow rate and the percentage of ingested gases with respect to the anode flow. These calculations confirm that the measured performance of a Hall thruster in the LVTF over these flow rates and pumping speeds is an adequate estimation of the performance that would be encountered in the space environment.

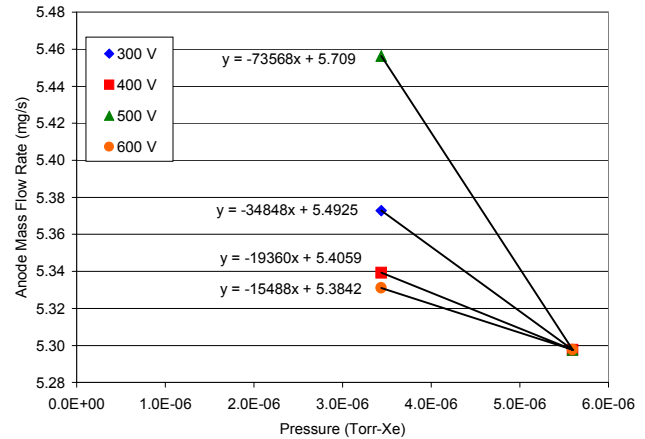


Figure 12 – Anode mass flow rate versus pressure (5.0 A).

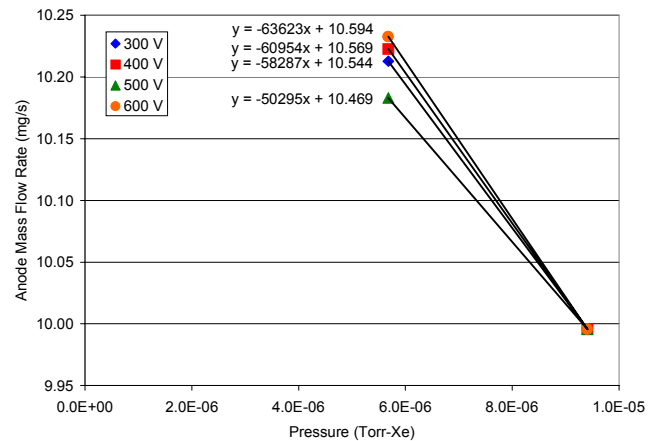


Figure 13 – Anode mass flow rate versus pressure (10 A).

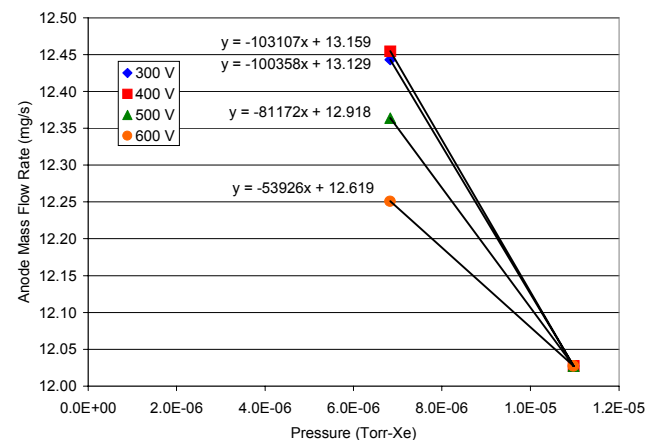


Figure 14 – Anode mass flow rate versus pressure (12.5 A).

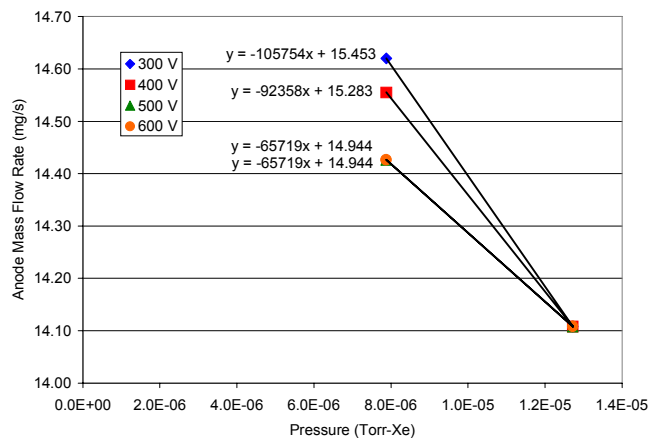


Figure 15 – Anode mass flow rate versus pressure (15.1 A).

Table 1 – Computed anode mass flow corrections as a function of discharge current and voltage with 7 cryopumps running.

Discharge Voltage [V]	5 A	10 A	12.5 A	15.1 A
	$\Delta\text{-mdot}$ (mg/s)	$\Delta\text{-mdot}$ (mg/s)	$\Delta\text{-mdot}$ (mg/s)	$\Delta\text{-mdot}$ (mg/s)
300	0.12	0.33	0.69	0.83
400	0.07	0.35	0.71	0.72
500	0.25	0.29	0.56	0.51
600	0.05	0.36	0.37	0.51
Average	0.12	0.33	0.58	0.64
% Error	82%	11%	29%	25%

Acknowledgments

We would like to dedicate this paper to the victims and their families of the terrorist attacks on the United States of America on September 11, 2001. Completing this manuscript during the week of the attacks was difficult, as it suddenly did not seem to be as important as it once did. Our hearts and prayers go out to all those who have been forever changed by this senseless tragedy.

This research was supported by the Air Force Office of Scientific Research grants F49620-00-1-0201 and F49620-01-1-0061 (Dr. Mitat Birkan is the contract monitor for both). The authors are greatly appreciative of this support.

References

- ¹ Kaufman, H. R., "Technology of Closed-Drift Thrusters," AIAA-83-1398, 19th Joint Propulsion Conference, Seattle, Washington, June 27-29, 1983.
- ² Gulczinski, F. S. and Gallimore, A. D., "Near Field Ion Energy and Species Measurements of a 5 kW Laboratory Hall Thruster " Journal of Propulsion and Power (AIAA), Vol. 17, No. 2, March-April 2001, 418-427.
- ³ Oleson, S. R., "Mission Advantages of Constant Power, Variable Isp Electrostatic Thrusters," AIAA-2000-3413, 36th Joint Propulsion Conference, Huntsville, AL, July 17-19, 2000.
- ⁴ Gefert, L. P., Hack, K. J., "Options for the Human Exploration of Mars Using Solar Electric Propulsion," AIP Conference Proceedings, No. 458, pp. 1275-1280, STAI-99, Nov 1999.
- ⁵ Dudzinski, L. A., Hack, K. J., Gefert, L. P., Kerslake, T. W., and Herston, A. W., "Design of a Solar Electric Propulsion Transfer Vehicle for a Non-Nuclear Human Mars Exploration Architecture, IEPC-99181, Proceedings of 26th International Electric Propulsion Conference," Kitakyushu, Japan, Oct. 17 – 21, 1999.
- ⁶ Jankovsky, R. S., Jacobson, D. T., Mason, L. S., Rawlin, V. K., Mantenieks, M. A., Manzella, D. H., Hofer, R. R., Peterson, P. Y., "NASA's Hall Thruster Program," AIAA-2001-3888, 37th Joint Propulsion Conference, Salt Lake City, UT, July 8-11, 2001.
- ⁷ Kim, V., "Main Physical Features and Process Determining the Performance of Stationary Plasma Thrusters," Journal of Propulsion and Power, Vol. 14, No. 5, pp. 736
- ⁸ Kim, S. W., and Gallimore, A. D., "Plume Study of a 1.35 kW SPT-100 Using an ExB Probe," AIAA 99-2423, 34th Joint Propulsion Conference, Los Angeles, CA, June 20 - 24, 1999.
- ⁹ King, L. B., and Gallimore, A. D., "Ionic and Neutral Particle Transport Property Measurements in the Plume of an SPT-100," (AIAA-96-2712): 32nd Joint Propulsion Conference, Orlando, FL, July 1996.
- ¹⁰ Fife, J. M., Hargus, W. A., Jaworski, D., Jankovsky, R., Mason, L., Sarmiento, C., Snyder, J. S., Malone, S. P., Haas, J., M., and Gallimore, A. D., "Spacecraft Interaction Test Results of the High Performance Hall System SPT-140," AIAA 2000-3521, 36th AIAA/ASME/SAE/ASEE Joint Propulsion, Huntsville, Alabama, 16-19 July 2000.
- ¹¹ Myers, R., and Manzella, D., "Stationary Plasma Thruster Plume Characteristics," IEPC 93-096, September 1993.
- ¹² Kusamoto, D., Mikami, K., Komurasaki, K., and Gallimore A. D., "Exhaust Beam Profiles of Hall Thrusters," Transactions of Japanese Society for Aeronautical and Space Sciences, Vol. 40, No.130, 1998, 238-247.
- ¹³ Randolph, *et al.*, "Facility effects on SPT thruster testing," IEPC-93-093, 23rd International Electric Propulsion Conference, Seattle, Washington, Sept. 13-16, 1993.
- ¹⁴ Marrese, C., Polk, J. E., King, L. B., Garner, C., Gallimore, A. D., Semkin, S., Tverdoklebov, S., and Garkusha, V., "Analysis of Anode Layer Thruster Guard Ring Erosion," Proceedings of the 24th International Electric Propulsion Conference, Moscow, Russia, Sept. 1995.
- ¹⁵ Gulczinski III, F. S., Examination of the Structure and Evolution of Ion Energy Properties of a 5 kW Class Laboratory Hall Effect Thruster at Various Operational Conditions, Ph.D. thesis, Dept. of Aerospace Engineering, The University of Michigan, Aug., 1999.
- ¹⁶ Hofer, R. R., Walker, M. L., and Gallimore, A. D., "A Comparison of Nude and Collimated Faraday Probes for Use with Hall Thrusters," IEPC-01-20, Proceedings of the International Electric Propulsion Conference, Pasadena, CA, October 14-19, 2001.
- ¹⁷ Haas, J. M., Gulczinski, F. S., Gallimore, A. D., Spanjers, G.G., Spores, R.A., "Performance Characteristics of a 5 kW Laboratory Hall Thruster," AIAA-98-3503, 34th Joint Propulsion Cleveland, OH, July 12-15, 1998.
- ¹⁸ Dushman, S., *Scientific Foundations of Vacuum Technique*, Vol. 4, Wiley, New York, 1958.

Appendix

Table A-1 – P5 Performance with four cryopumps operating in the LVTF.

Vd (V)	Id (A)	Pd (Watts)	Anode Flow (mg/s)	Cathode Flow (mg/s)	Vim (V)	Iim (A)	Vom (V)	Iom (A)	Pmag (Watts)	Vhtr (V)	Ihtr (A)	Vc-g (V)	Pressure (Torr-Xe)	Thrust (mN)	Anode Isp (sec)	Anode Eff	Total Isp (sec)	Total Eff
300.0	4.86	1458	5.30	0.60	4.75	2.24	2.65	1.01	13.32	6.3	5.99	-23.5	5.6E-06	82.3	1584	0.44	1423	0.39
400	4.76	1904	5.30	0.60	5.28	2.50	3.31	1.26	17.37	6.4	5.99	-24.0	5.6E-06	98.6	1898	0.48	1704	0.43
500	5.00	2500	5.30	0.60	7.46	3.52	3.96	1.51	32.24	6.4	5.98	-23.1	5.6E-06	111.9	2154	0.47	1934	0.42
600	5.24	3144	5.30	0.60	7.79	3.51	7.90	2.95	50.65	6.5	6.00	-24.2	5.6E-06	126.8	2439	0.48	2190	0.43
299.8	9.92	2974	10.00	0.60	9.68	4.00	5.33	2.01	49.43	7.6	6.00	-22.9	9.4E-06	170.5	1739	0.49	1640	0.45
400	9.98	3992	10.00	0.60	11.18	4.51	5.35	2.01	61.18	7.6	6.00	-23.5	9.4E-06	207.5	2116	0.54	1996	0.50
500	10.04	5020	10.00	0.60	11.78	5.01	5.28	2.01	69.63	7.5	6.00	-23.9	9.4E-06	237.1	2418	0.56	2281	0.52
600	10.18	6108	10.00	0.60	18.34	6.51	7.01	2.52	137.06	7.7	6.00	-25.1	9.4E-06	266.7	2720	0.58	2566	0.54
300.0	12.42	3726	12.03	0.60	18.21	6.00	5.74	1.99	120.68	8.4	6.00	-23.9	1.1E-05	208.7	1768	0.49	1684	0.45
400	12.48	4992	12.03	0.60	20.38	6.51	5.77	1.99	144.16	8.4	6.00	-24.6	1.1E-05	254.7	2158	0.54	2056	0.50
500	12.48	6240	12.03	0.60	18.91	6.00	5.80	1.99	125.00	8.4	6.00	-24.7	1.1E-05	290.3	2460	0.56	2343	0.52
600	12.60	7560	12.03	0.60	26.82	7.99	5.94	2.01	226.23	8.5	6.00	-25.4	1.1E-05	323.7	2743	0.58	2613	0.53
300.0	15.12	4536	14.11	0.60	17.85	6.00	5.66	2.01	118.48	9.0	6.00	-25.7	1.3E-05	254.2	1837	0.51	1762	0.47
400	15.10	6040	14.11	0.60	20.28	6.52	5.73	2.01	143.74	9.1	6.00	-26.6	1.3E-05	309.8	2238	0.56	2147	0.53
500	15.00	7500	14.11	0.60	21.12	7.00	5.40	1.99	158.59	9.2	6.02	-27.9	1.3E-05	356.4	2575	0.60	2470	0.56
600	15.32	9192	14.11	0.60	29.73	8.51	5.90	2.01	264.86	9.2	6.00	-27.4	1.3E-05	399.4	2886	0.61	2768	0.57

Table A-2 – P5 performance with seven cryopumps operating in the LVTF.

Vd (V)	Id (A)	Pd (Watts)	Anode Flow (mg/s)	Cathode Flow (mg/s)	Vim (V)	Iim (A)	Vom (V)	Iom (A)	Pmag (Watts)	Vhtr (V)	Ihtr (A)	Vc-g (V)	Pressure (Torr-Xe)	Thrust (mN)	Anode Isp (sec)	Anode Eff	Total Isp (sec)	Total Eff
299.9	4.86	1458	5.37	0.60	4.67	2.24	2.598	1.01	13.08	6.4	6.00	-20.8	3.4E-06	85.9	1630	0.47	1466	0.42
400	4.76	1904	5.34	0.60	5.20	2.50	3.249	1.26	17.09	6.4	6.00	-21.6	3.4E-06	101.7	1942	0.51	1746	0.45
500	5.00	2500	5.46	0.60	7.51	3.51	3.92	1.51	32.28	6.4	6.00	-21.4	3.4E-06	116.8	2182	0.50	1966	0.44
600	5.24	3144	5.33	0.60	7.88	3.51	7.91	2.95	50.99	6.4	6.00	-21.8	3.4E-06	131.1	2507	0.51	2253	0.45
300.0	9.92	2976	10.21	0.60	8.75	4.00	5.20	2.01	45.45	7.5	6.00	-20.2	5.7E-06	174.7	1743	0.50	1646	0.47
400	9.98	3992	10.22	0.60	10.53	4.51	5.24	2.01	58.02	7.6	6.00	-20.8	5.7E-06	212.4	2118	0.55	2001	0.51
500	10.04	5020	10.18	0.60	12.44	5.01	5.28	2.01	72.94	7.6	6.00	-20.9	5.7E-06	238.9	2391	0.56	2258	0.52
600	10.18	6108	10.23	0.60	18.02	6.51	6.81	2.53	134.54	7.6	6.00	-22.1	5.7E-06	268.3	2673	0.58	2525	0.53
300.0	12.42	3726	12.44	0.60	13.04	5.01	5.3	1.98	75.82	8.2	6.01	-21.9	6.8E-06	215.2	1763	0.50	1682	0.47
400	12.48	4992	12.45	0.60	18.15	6.51	5.33	1.99	128.76	8.3	6.01	-23.3	6.8E-06	260.5	2132	0.55	2034	0.51
500	12.48	6240	12.36	0.60	17.7	6	5.41	1.99	116.97	8.3	6.01	-23.2	6.8E-06	298.3	2459	0.58	2345	0.54
600	12.60	7560	12.25	0.60	26.62	7.99	5.55	1.99	223.74	8.4	6.01	-23.7	6.8E-06	329.3	2740	0.59	2612	0.54
300.1	15.12	4538	14.62	0.60	17.05	6	5.53	1.99	113.30	9.0	6.01	-24.4	7.9E-06	253.8	1770	0.49	1700	0.45
400	15.10	6040	14.56	0.60	19.93	6.51	5.58	1.99	140.85	9.1	6.01	-25.6	7.9E-06	309.7	2169	0.55	2083	0.51
500	15.00	7500	14.43	0.60	22.61	6.99	5.66	1.99	169.31	9.1	6.00	-25.9	7.9E-06	354.2	2503	0.58	2403	0.54
600	15.34	9204	14.43	0.60	30.44	8.51	5.89	1.99	270.77	9.2	6.00	-27.1	7.9E-06	396.5	2802	0.59	2690	0.55